

## Projectile Accelerator Prototype using Electromagnetic Fields

John Castillo, Nathalia Gama and Dario Amaya  
Virtual Applications Group (GAV), Nueva Granada Military University (UMNG),  
Bogota, Colombia

**Abstract:** Typically, the firing of a projectile is carried out by chemical means, through the reactions of the gunpowder or by means of the use of compressed air. These methods have certain disadvantages such as noise and friction losses, low speeds, among others. An alternative method for the firing of a projectile is the accelerator of electromagnetic fields which allows the launch, through the magnetic field generated in a solenoid which facilitates to obtain much higher speeds. In this study, we present the results obtained in the design and implementation of a prototype based on the cannon-coil principle. In the first part of the research, a short introduction is made to the theory of electromagnetic launchers and it outlines the state of the art of this type of launchers and its applications in the militia and in the civil sector. The second part presents the design process and the subsequent implementation of the electromagnetic cannon. Consequently, the analysis of the behavior of the system is developed and the results obtained from the firing tests performed with the prototype are shown.

**Key words:** Cannon-coil, electromagnetic launchers, electromagnetic forces, solenoid, armament, prototype

---

### INTRODUCTION

Electro Magnetic Launchers (EMLs) are defined as devices capable of converting electromagnetic energy into kinetic energy, achieving the movement of a projectile along a defined path. The cannon-coil, rail gun, electro-thermochemical weapons and electrostatic weapons are the main examples of EMLs (Balıkcı, 2008). In the last decades, special interest has been given in this type of projectile accelerators given the disadvantages of the traditional methods based on the forces generated by the pressure of gases in the chemical reactions of the gunpowder or by means of compressed air. These firing methods produce a large number of gases and sounds that are easily perceptible over long distances. In addition, they require large steel structures to withstand the high pressures given in their operation. Some of the advantages of electromagnetic launchers compared to those operated by conventional means is that they can accelerate projectiles at much higher speeds, the firing process is practically free of friction between the projectile and the armature, the load can be easily installed and the system in general has a high-energy conversion efficiency (Zhang *et al.*, 2012). NASA, to drive long models of hyper-speed for flight tests has taken the great advantages presented by the electromagnetic launchers. NASA's cannon-coil was designed to accelerate a mass

from 14 kg to 6 km/sec. The importance of this development lies in being able to use the EML for aeronautical research in the upper atmosphere and eventually to locate small rockets in the low orbit in earth (Schroeder *et al.*, 1989).

The electromagnetic accelerators base their operation on the magnetic field generated in an air core solenoid through which flows a current flow due to a potential change (Sears *et al.*, 1994). Carl Friedrich Gauss formulated the mathematical proofs of the electromagnetic effect used by the cannon-coil. If a short current pulse passes through the coil, the projectile will accelerate toward the center of the coil. When the current pulse is interrupted before the projectile reaches the center of the coil, the projectile is thrown from the opposite end of the coil and will continue to accelerate throughout its solenoid exit path (Furuya and Uehara, 2009). During the trajectory of the projectile, the force acting on it varies with the position of the projectile (Hou *et al.*, 2012). The force acting on the projectile, per unit volume thereof is given by Eq. 1:

$$F = M_m \frac{dH}{dx} \quad (1)$$

Where:

$M_m$  = The intensity of magnetization

$H$  = The magnetic field strength

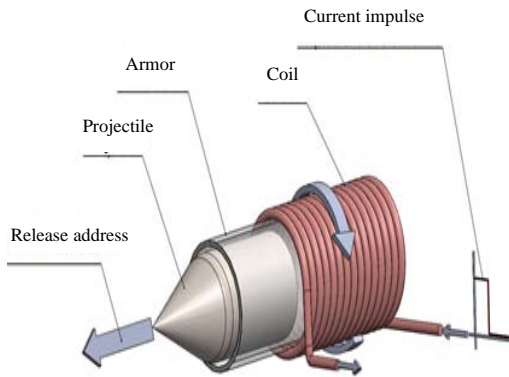


Fig. 1: Reluctance cannon-coil system

The magnetization of the projectile is determined by the properties of the material of which it is constituted while the gradient of the magnetic field is determined by the induced current and the structure (Serway, 2009). The magnetic induction intensity at any point inside the accelerator is given by Eq. 2:

$$\oint \mathbf{B} \times d\mathbf{s} = \mathbf{B}l = \mu_0 \mathbf{N}I \quad (2)$$

$$\mathbf{B} = \mu_0 n\mathbf{I}$$

Where:

$\mu_0$  = Permeability index

$I$  = Induced current

$n$  = Number of turns per unit length

The EML used in this research is the reluctance coil cannon in which the projectile is a piece of ferromagnetic material that can be accelerated at high speed (Hou *et al.*, 2012). Reluctance is the resistance to the creation of magnetic flux in the material around the coil, the electromagnetic material inside the coil reduces this reluctance (Bresie and Andrews, 1991). Its operating principle is shown in Fig. 1. In addition to the reluctance coil, there are also, the induced pulse, the induced wave and the helical wave of brushes whose processing has a higher degree of complexity (Braam, 2007; Kaye *et al.*, 2002).

More specifically, in comparison to the other EMLs, the coil cannon allows the launching of larger mass projectile is highly efficient and achieves much higher firing speeds, similarly reducing mechanical stress and distributing thrust more efficiently (Hou *et al.*, 2012; Levi *et al.*, 1991). Compared with conventional methods, the mass of the ammunition is reduced, since, the use of gunpowder will be omitted. The weight of the arms is reduced due to the change in the shot conditions which

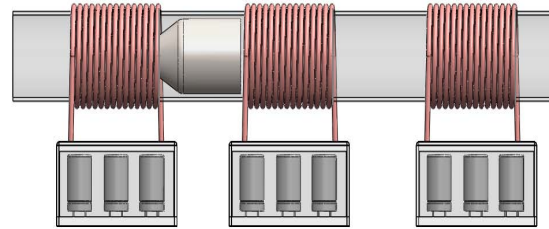


Fig. 2: Basic control circuit diagram

do not require high pressure, avoiding the inclusion of different moving parts to the projectile and reducing in turn the level of the noise produced in the shot process. Figure 2 shows a basic schematic of the operation of the coil cannon from pulse generation to the production of the shot. The current impulse supplied to the coil comes from the process of loading and unloading the power banks, composed of several arrangements of high power electrolytic capacitors located in series. All the developed variations of coil cannon have certain common elements as they are a power source, a coil of conduction and a control circuit (Braam, 2007).

A multi-stage coil cannon is composed of several solenoids each powered by its own capacitor bank. An activation circuit for each state allows interleaving of the coils to achieve acceleration of the projectile throughout all stages (Su *et al.*, 2012). From the design parameters of the coils, the capacitor bank and the activation times of these will depend on the projectile reaching a high firing speed (Yanjie *et al.*, 2009).

The principle of operation of the cannon-coil has a wide application in the military area: like support to naval arms of long range and catapult launchers of great mass, among others. However, it also presents developments in the industry in precision stop devices in the area of transport in low and high-speed trains (Kaye *et al.*, 2002), electromagnetic tools and actuators (Slade, 2005) and even future space applications such as launching vehicles to the space and positioning of orbiting satellites that have been given an initial velocity by means of a long reluctance accelerator. After exiting the accelerator, the vehicle can ignite its propellers until reaching the orbit which would mean a significant fuel saving (Waindok and Mazur, 2009). In the latter case, the energy for a launch of this nature would be of the order of 2000 MJ with an electric power of approximately 2 MW which would have to be supplied by approximately 400 power bank and coils modules (Turman, 1999).

Some of the work that preceded this research were those developed at Sandia Laboratories by researchers

at the Massachusetts Institute of Technology where experiments were conducted with five-stage inductive coil cannons that could accelerate 10-15 kg shells at speeds in excess of 1 km/sec (Zhang *et al.*, 2012). More specific works on the reluctance coil cannon are presented by Slade (2005). Where a unified physical model of the reluctance accelerator is developed, developing a dynamic model using the Lagrange approach, obtaining a clear illustration of the energy exchange to and from the projectile which provides a good understanding of the electrical stress to which the coils of the barrel are subjected as well as their mechanical behavior. The reluctance coil is conducive to its implementation in hostile environments, underwater or space applications because its operating system does not require sliding contacts or flexible cables. By Bresie and Andrews (1991), the design parameters of this type of accelerator, some control and modeling methods of the system whose nature is highly non-linear is presented. By Waindok and Mazur (2009), we present the design of a reluctance coil cannon where the force and kinetic energy of the projectile are constant values and the dimensions of the coil are variable as well as the length of the projectile. Parameters that are obtained in order to optimize the behavior of the coil cannon. The same researchers, feature by Waindok and Mazur (2011), a new mathematical model of coil reactance cannon of three states. The model takes into account the mutual inductances in the accelerator that have influence on the current waves in the coils. They also use the finite element method to calculate model parameters.

## MATERIALS AND METHODS

This study explains the methodology used for the design of the coil and the capacitor bank. The prototype implemented in a single-stage system that allows the launching of two different types of projectiles, one cylindrical and one spherical. The subsequent construction of the coil and elaboration of the battery bank is done based on the design calculations elaborated in this study. This is done in order to compare the actual performance of the projectile with its theoretical performance in the results stage, thus, obtaining a feasible approximation of the amount of energy lost in the shot process.

**Design of the air core solenoid:** The following are the variables that were established as initial design

parameters for the calculation and subsequent manufacture of the solenoid. The value of the shot speed or mouth speed is established based on the study of the state of the art performed in the first stage of the work. The value selected is an average value for launching a projectile in real military applications:

- Tripping speed: 22.8 m/sec
- Maximum current in the system: 640 A
- Mass of the projectile: 0.0329 kg
- Voltage applied in the system: 650 V

As it is observed in Eq. 3, the time required for the projectile to fire is calculated by the time it takes to pass the half of the solenoid, so that, the shot process can be carried out in accordance with (Furuya and Uehara, 2009):

$$t_0 = \frac{2d}{v} \quad (3)$$

Where:

- d = The length of the solenoid
- V = The shotter speed

And where  $t_0$  is the time that the current pulse in the coil must last for the projectile to reach the desired output velocity and the solenoid reluctance value does not cause the projectile to be permanently attracted by the magnetic field generated in the coiled. Starting from  $t_0$ , the values for the magnetic inductance field as well as the inductance and resistance of the coil are calculated. Equation 4 and 5 show the force components that take place during the shot process:

$$F = m \times a \quad (4)$$

$$F_m = B \times I \times d \quad (5)$$

Where :

- F = The required force for the selected projectile to reach the required firing speed
- B = The magnetic inductance
- I = The maximum current supported by the system
- $F_m$  = The magnetic force due to the magnetic inductance

Equation 4 and 5 are equated and clearing B:

$$B = 3.94 \text{ T}$$

Using Eq. 2 its calculated the number of turns required in the coil:

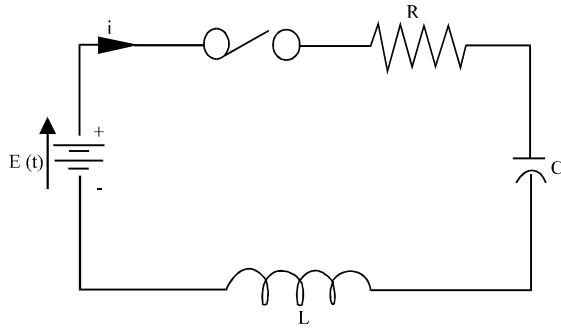


Fig. 3: Representation of the cannon-coil system as an RLC circuit

Table 1: Characteristics of the solenoid

Features solenoid	Values
$\mu_0$	1.25664E-6 Wb/Am
Number of turns per layer	61.72839506
Total turns number	497
Solenoid length	0.1 m
Inductance	695.58 $\mu$ H
<b>Dimensions cross section of the solenoid (mm)</b>	
Initial diameter (core)	20 mm
Wire diameter	1.62 mm
Number of layers	7
Diameter cross section	42.68 m
Cross sectional area (mm <sup>2</sup> )	1430.667471 mm <sup>2</sup>
<b>Coil resistance</b>	
Coefficient of resistivity	1.71E <sup>8</sup>
Length of winding wire	54.309 m
Wire transverse area	2.0612E <sup>6</sup>
Coil resistance	0.896 $\Omega$

$$N = 490.2$$

Finally, using Eq. 6 which shows the Wheeler (1982) equation, we obtain the inductance value to finally, represent the coil cannon system as an electric circuit RLC as shown in Fig. 3:

$$L = 0.394 \frac{a^2 N^2}{9a+10l} \mu\text{H} \quad (6)$$

$$L = 695.58 \mu\text{H}$$

We proceeded to construct the air core solenoid that meets the characteristics determined in the design stage. Additional characteristics of the solenoid are shown in Table 1.

**Design of the battery bank:** The design of the battery bank is also based on the design parameters set out in the first part of the methodology. The magnitude of charge in a set of capacitors is the same when they are in series or in parallel, however, the maximum voltage can be reached by the arrangement of the capacitors in series as shown in Eq. 7:

$$V_T = V_1 + V_2 + V_3, \dots, V_n \quad (7)$$

As an additional design parameter, the characteristics of the capacitors acquired for the development of the project were established where each capacitor has the following characteristics:

$$\text{Capacitance} = 10000 \mu\text{F} \rightarrow 0.001 \text{ F Voltage} = 80 \text{ V}$$

Therefore, from Eq. 7 with equal voltages, we get:

$$V_1 = V_2 = V_3 = \dots, V_n \quad (8)$$

$$V_T = V_c N_c$$

Where  $V_c$  and  $N_c$  correspond to the voltage of the capacitors and the number of capacitors, respectively. Fulfilling the 640 V requirement of Eq. 8 gives:

$$640 = 80 N_c$$

$$N_c = 8$$

$$C_1 = C_2 = C_3 = \dots, C_n \quad (9)$$

$$\frac{1}{C_{eq}} = \frac{1}{C_{ap}} \times N_c$$

Placing eight capacitors in series fulfills the voltage requirement. Equation 9 allows the calculation of the equivalent capacitance starting from the capacitance required and the number of capacitors required by the system. Setting the required capacitance value equal to 0.01 and replacing these values in Eq. 9 gives:

$$\frac{1}{C_{eq}} = \frac{1}{0.01} \times 8$$

$$C_{eq} = 0.00125$$

Since, the capacitance requirement is equal to 0.0025 F, a capacitor arrangement is made to increase the capacitance to the required value. For this the following proportion is used knowing that the capacitance in parallel capacitors is added:

$$C_D = C_{eq} \times N_{cp} \quad (10)$$

Where  $C_D$ ,  $C_{eq}$ ,  $N_{cp}$  correspond to desired capacitance, previous equivalent capacitance and number of capacitors in parallel per array, respectively. Obtaining this way:

$$0.0025 = 0.00125 \times N_{cp}$$

$$N_{cp} = 2$$

Taking into account this design concept, we obtain an energy bank of 8 capacitors in series

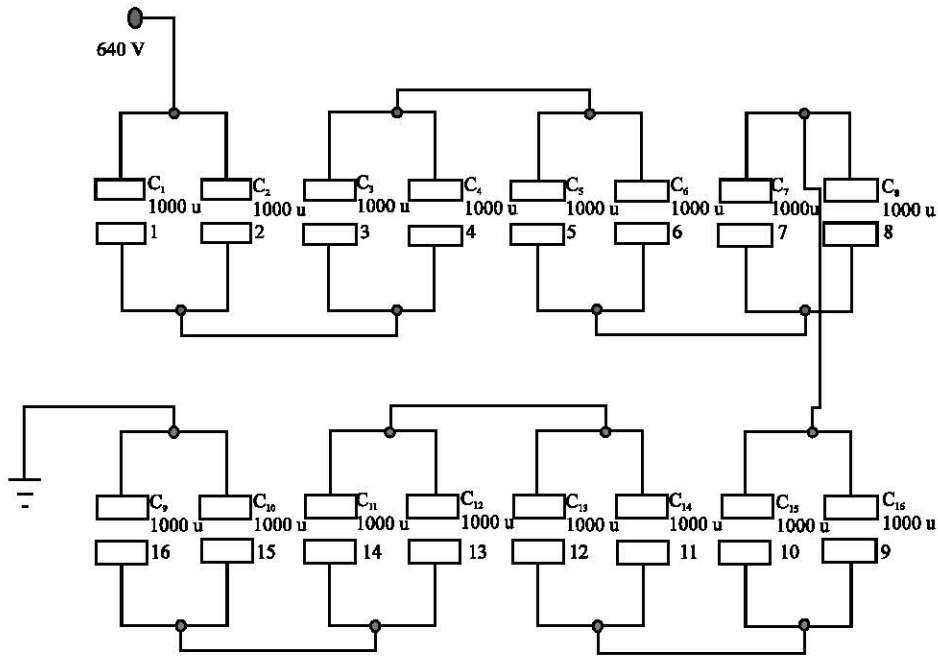


Fig. 4: Battery bank designed

each of 0.002F, obtained from 2 capacitors in parallel. Figure 4 shows a diagram of the battery bank designed.

**RESULTS AND DISCUSSION**

**Mathematical analysis of system behavior:** Assuming system as an RLC circuit, it part of differences equation to analyze the behavior of this one during the process of firing of the projectile. The differential equation of the system is shown in Eq. 8 which expresses the energy inputs of the three main components of the system: the inductance and resistance of the solenoid and the equivalent capacitance of the battery bank:

$$L \frac{d^2 i}{dt^2} + R_1 \frac{di}{dt} + \frac{1}{C} \int i dt = E \tag{11}$$

Solving the equation of the second order gives:

$$L m^2 + R_m + \frac{1}{C} = 0 \tag{12}$$

$$m_1 = -a + \sqrt{a^2 - w^2}$$

$$m_2 = -a - \sqrt{a^2 - w^2}$$

Solving the equation yields complex roots that result in a sub-damped response in current behavior over time.

This response depends on the relationship between the variables R, L and C. For a system with a sub-damped response, the general solution is given by Eq. 13:

$$i(t) = e^{at} (A \cos wt + B \sin wt) \tag{13}$$

Where:

$$a = \frac{R}{2L}$$

$$w = \sqrt{\frac{1}{LC} - \frac{R^2}{4L^2}}$$

Where w is the natural frequency of the system and variables A and B are calculated under the preset design conditions:

$$i(t) = 0 \text{ when } t = t_0$$

$$i'(t) = 0 \text{ when } t = \frac{t_0}{2}$$

The first condition indicates that a current value equal to 0 is estimated at time  $t_0$  in order to achieve that the projectile reaches the desired output velocity, likewise preventing the projectile from being permanently attracted by the magnetic field generated in the coil. The second condition states that it is sought to obtain the maximum value of current in a time equal to  $t_0/2$ . The derivative of the current corresponds to the slope of the graph, when establishing this slope as 0 is fulfilled at that instant

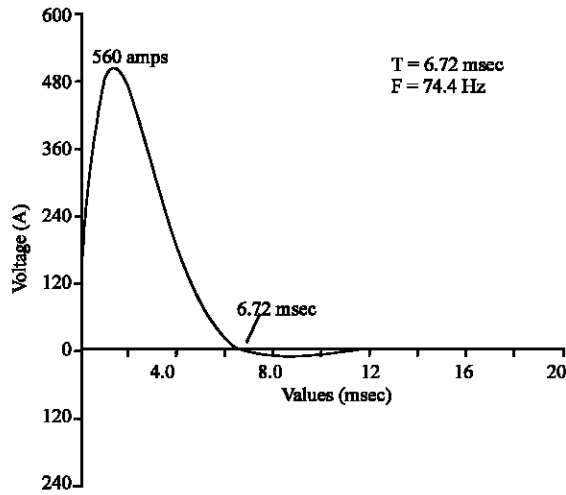


Fig. 5: Initial response of the RLC system;  $V = 650\text{ V}$ ,  $R = 850\text{ m}\Omega$ ,  $C = 2.50\text{ mF}$ ,  $L = 800\text{ }\mu\text{H}$



Fig. 6: Designed projectile accelerator

of time will obtain the maximum value of the current that will immediately begin to decrease until reaching 0 in  $t_0$ . Figure 5 shows the change in current in the coil during the initial response. Note the value of  $t_0 = 6.72\text{ msec}$ , the instant where the initial pulse of current in the coil ends and the projectile reaches the distance  $d$ , allowing it to be launched with the desired trip speed.

**Construction of the prototype:** Under the design parameters established in the methodology, we proceed to the prototype of a one-stage cannon-coil composed by a bank of capacitors an air core winding, the PVC reinforcement and the metal projectile of 20 mm in diameter. Figure 6 shows the manufactured prototype of the projectile accelerator. The throwing angle is preset at  $45^\circ$  from the horizontal.

Table 2 shows the structural parameters of the armature used and the power bank with which the prototype of the cannon-coil was tested. The experimental tests consisted in measuring the launch distance and the firing speed to compare these magnitudes with those obtained theoretically. The difference in the obtained results allows to establish the energy losses during the

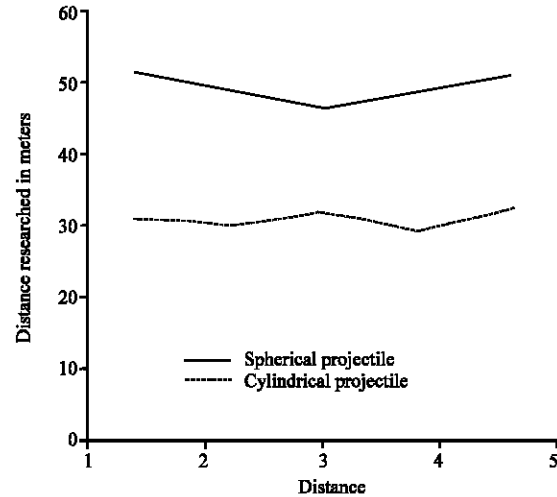


Fig. 7: Results of the distance and speeds reached in the experimental tests

Table 2: Structural parameters armature and energy bank

Type of material	PVC
<b>Armor</b>	
External diameter	22 mm
Internal diameter	20 mm
Length	250 mm
<b>Power bank</b>	
Number of arrangements	8
Condensers by arrangement	2-80 V c/u
Equivalent capacitance	0.0025 F
Input voltage	640 V

Table 3: Shot with spherical projectile; projectile mass: 32.46 g

Number shot	Distance experimental reach (m)	Speed in mouth (from experimental distance) at
		$45^\circ$ (m/sec)
1	53.40	23.01
2	51.10	22.50
3	48.50	21.90
4	50.68	22.40
5	52.97	22.90

Table 4: Shot with cylindrical projectile; projectile mass: 46 g

Number shot	Distance experimental reach (m)	Speed in mouth (from experimental distance) at
		$45^\circ$ (m/sec)
1	33.0	18.1
2	32.0	17.8
3	33.8	18.3
4	31.2	17.6
5	34.5	18.5

shot process. Table 3 and 4 show the results of a series of 5 shots with the manufactured prototype. These values will also depend on the geometry of the projectile launched and its mass. The prototype was tested with a spherical projectile and a cylindrical projectile.

Figure 7 summarizes the results of the distances and speeds reached in the experimental tests, comparing the

launches with spherical projectile with those made with cylindrical projectile using the same prototype and the same energy impulse.

The results obtained are a very good first approximation to the behavior of a major electromagnetic launcher and allow the study and analysis of the behavior of the system from the construction of a prototype. This analysis can be extrapolated to a larger scale, providing a fundamental basis for the construction of weapons based on the cannon-coil principle. The advances developed in this research present a significant support to the defense sector as they raise the groundwork for future implementations of coil guns within the military artillery and place the national army at the forefront of technology and innovation worldwide.

Comparing the results obtained with the calculations elaborated in the design stage, it can be determined that the prototype uses approximately 70% of the energy generated by the system to launch the projectile, representing 30% in frictional losses during the passage through armor and heat generation. Constructing the prototype, the distances of the calculated projectiles were reached with a 15% margin of error. Currently, the best launch reaches a distance of more than 50 m in parabolic shot at 45°.

### CONCLUSION

The theoretical calculations are far from reality when losses are not considered; In this research, we tried to adjust a percentage proportional to the performance of each experiment which allowed us to get close enough to the actual results. However, there are still losses due to more complex factors as the differential variation of the coefficient of permeability inside the coil which presents a fluctuation between the coefficient of permeability of the air that is equal to  $1.26E^{-6}$  and the coefficient of permeability of the steel that is estimated in 2 can affect in excess of the final result of calculating the resulting force.

### RECOMMENDATIONS

It is recommended to manufacture a new winding with a thinner wire gauge which will optimize the number of turns per unit length in the solenoid. However, the wire must be able to withstand the high peak amperage found in the circuit which repeatedly exceeds 500 A.

As a future research, we propose the implementation of two or three additional stages in the projectile

accelerator. The use of several stages allows the achievement of higher launch speeds as the projectile receives during its tour of the armor various several “thrust” that allows it to achieve greater accelerations and therefore, shots with greater power and range.

### REFERENCES

- Balikci, A., 2008. High velocity linear induction launchers. *Intl. J. Impact Eng.*, 35: 1405-1409.
- Braam, D., 2007. Design and construction of a pulsed linear induction motor. MSc Thesis, Department of Mechanical Engineering, University of Cape Town, Cape Town, South Africa.
- Bresie, D.A. and J.A. Andrews, 1991. Design of a reluctance accelerator. *IEEE. Trans. Magn.*, 27: 623-627.
- Furuya, S. and Y. Uehara, 2009. Coilgun driven by commercial power supply. *Proceedings of the IEEE International Conference on Plasma Science-Abstracts (ICOPS 2009)*, June 1-5, 2009, IEEE, San Diego, California, USA., ISBN:978-1-4244-2617-1, pp: 1-1.
- Hou, Y., Z. Liu, J.M. Ouyang and D. Yang, 2012. Parameter settings of the projectile of the coil electromagnetic launcher. *Proceedings of the 16th International Symposium on Electromagnetic Launch Technology (EML)*, May 15-19, 2012, IEEE, Beijing, China, ISBN:978-1-4673-0306-4, pp: 1-4.
- Kaye, R.J., B.N. Turman and S.L. Shope, 2002. Applications of coilgun electromagnetic propulsion technology. *Proceedings of the 25th International Power Modulator Symposium on High-Voltage Workshop*, June 30-July 3, 2002, IEEE, Hollywood, California, USA., ISBN:0-7803-7540-8, pp: 703-707.
- Levi, E., J.L. He, Z. Zabar and L. Birenbaum, 1991. Guidelines for the design of synchronous-type coilguns. *IEEE. Trans. Magn.*, 27: 628-633.
- Schroeder, J.M., J.H. Gully and M.D. Driga, 1989. Electromagnetic launchers for space applications. *IEEE. Trans. Magn.*, 25: 504-507.
- Sears, W.F., F.A. Lewis and R.A. Freedman, 1964. *University Physics*. Vol. 2, Addison-Wesley Pub. Co., Boston, Massachusetts, Pages: 1028.
- Serway, J., 2009. *Physics for Science and Engineering with Modern Physics*. Cengage Learning, Mexico,.
- Slade, G.W., 2005. A simple unified physical model for a reluctance accelerator. *IEEE. Trans. Magn.*, 41: 4270-4276.

- Su, Z., W. Guo, B. Zhang, M. Li and C. Zhang *et al.*, 2012. The feasibility study of high-velocity multi-stage induction coilgun. Proceedings of the 16th International Symposium on Electromagnetic Launch Technology (EML), May 15-19, 2012, IEEE, Beijing, China, ISBN:978-1-4673-0306-4, pp: 1-4.
- Turman, B.N., 1999. Coilgun launcher for nanosatellites. Sandia National Labs., Albuquerque, New Mexico, Livermore, California. <https://www.osti.gov/scitech/biblio/5039>.
- Waindok, A. and G. Mazur, 2009. A mathematical and physical models of the three-stage reluctance accelerator. Proceedings of the 2nd International Students Conference on Electrodynamic and Mechatronics (SCE 11'09), May 19-21, 2009, IEEE, Silesia, Poland, ISBN:978-1-4244-3897-6, pp: 29-30.
- Waindok, A. and G. Mazur, 2011. Mutual inductances in a mathematical model of the three-stage reluctance accelerator. Proceedings of the 3rd International Students Conference on Electrodynamics and Mechatronics (SCE III), October 6-8, 2011, IEEE, Opole, Poland, ISBN:978-1-4244-9694-5, pp: 115-118.
- Wheeler, H.A., 1982. Inductance formulas for circular and square coils. Proc. IEEE., 70: 1449-1450.
- Yanjie, C., L. Wenbiao, L. Ruifeng, Yi, Z. and Z. Bengui, 2009. Study of discharge position in multi-stage synchronous inductive coilgun. IEEE. Trans. Magn., 45: 518-521.
- Zhang, T., W. Guo, Z. Dong, Y. Chen and M. Li *et al.*, 2012. Experimental results from a 4-stage synchronous induction coilgun. Proceedings of the 16th International Symposium on Electromagnetic Launch Technology, May 15-19, 2012, IEEE, Beijing, China, ISBN:978-1-4673-0306-4, pp: 1-5.